International Journal of Electrical and Computer Engineering (IJECE)
Vol. 11, No. 6, December 2021, pp. 4865~4880
ISSN: 2088-8708, DOI: 10.11591/ijece.v11i6.pp4865-4880

Decentralised PI controller design based on dynamic interaction decoupling in the closed-loop behaviour of a flotation process

N. Tshemese-Mvandaba, R. Tzoneva, M. E. S. Mnguni
Department of Electrical, Electronics and Computer Engineering, Faculty of Engineering and the Built Environment, Cape Peninsula University of Technology, South Africa

Article Info

Article history:

Received Aug 3, 2020
Revised May 17, 2021
Accepted Jun 1, 2021

Keywords:

Closed-loop performance
Column flotation process modelling
Controller design
Model decoupling
Multivariable systems
Pole placement

ABSTRACT

An enhanced method for design of decenralised proportional integral (PI) controllers to control various variables of flotation columns is proposed. These columns are multivariable processes characterised by multiple interacting manipulated and controlled variables. The control of more than one variable is not an easy problem to solve as a change in a specific manipulated variable affects more than one controlled variable. Paper proposes an improved method for design of decentralized PI controllers through the introduction of decoupling of the interconnected model of the process. Decoupling the system model has proven to be an effective strategy to reduce the influence of the interactions in the closed-loop control and consistently to keep the system stable. The mathematical derivations and the algorithm of the design procedure are described in detail. The behaviour and performance of the closed-loop systems without and with the application of the decoupling method was investigated and compared through simulations in MATLAB/Simulink. The results show that the decouplers - based closed-loop system has better performance than the closed-loop system without decouplers. The highest improvement (2 to 50 times) is in the steady-state error and 1.2 to 7 times in the settling and rising time. Controllers can easily be implemented.

Corresponding Author:

Nomzamo Tshemese-Mvandaba
Department of Electrical and Computer Engineering
Faculty of Engineering and the Built Environment
Cape Peninsula University of Technology
Symphony Way, Bellville, South Africa
Email: tshemesen@cput.ac.za, nltshemese@gmail.com

1. INTRODUCTION

The flotation column is a multivariable process whose main control objective is to guarantee that the metallurgical performance does agree with the process operation, expressed by the grade and the recovery of the valuable mineral in the concentrate [1], [2]. There is a long history of utilisation of this process and a lot of research and development works have been carried out [2]. The paper [3], states that the flotation process is still not fully understood, and remains quite inefficient if its proper control is overlooked. Column flotation is industrially known as a continuous solid to solid separation process [4] performed in a vessel where a three-phase system is present: solid particles, air bubbles, and water [1], [5], [6]. According to [7], this pulp is conditioned earlier with the controlled addition of small quantities of specific chemical reagents to promote the selective formation of aggregates between solid particles of a given composition and the air bubbles. The process is normally started in the presence of the feed inlet (liquid), air is injected continuously in the pulp where some air bubbles are formed [4], [8], [9]. The main control objective of the column flotation process is

to improve the metallurgical execution to ensure that the column operation comes to the reference values necessary for the specified recovery and position of the concentrate stream, [10]-[12]. Since hydrodynamic variables are closely related to the metallurgical and economic performances of the flotation unit, the implementation of intelligent control strategies is crucial to optimize its operation [2], [13], [14]. Tang *et al.* [15] presents some investigations to achieve the desired performance of networked flotation processes using robust model predictive control (RMPC). Another common way of controlling the process systems with strong nonlinearities in the model-based predictive controller also known as MPC [7], [16]-[18]. There are many other strategies used for industrial process controller design such as artificial neural network (ANN) based controller [19], different optimization solutions as presented by [20], [21] using Pareto-based method, and radial basis function neural network metamodel respectively. Fuzzy predictive control [8] and internal model control (IMC), are discussed in [22].

While there are still some additions, it is acknowledged that after the first attempts done in the late eighties, significant progress in column flotation dynamic simulation has been made. According to the literature many good optimization techniques can be used for multi-objective systems [20], [21], but the cost associated with multivariable systems is still a major problem that prevents the general use of optimization techniques. Then again, many controller design methods are applied and published such as ANN, MPC, different optimization methods, and fuzzy logic control which seems to be the successful techniques [8], [19], [20], [23]. However, when it comes to industrial application, many industries still use proportional integral (PI) or proportional integral derivative (PID) controllers [24] as one of the first developed control strategies with simple structure and well-known tuning rules. This makes them easy to maintain dominance in practical engineering applications for several decades [24], [25]. Nevertheless that more advanced control algorithms have been developed, the PI or PID controllers are always preferred unless they do not give satisfactory performance [24]. Ogunnaike *et al.* [23] emphasises important aspects of the industrial control systems implementation, which means how the actual measurements from the process to the controller and back are performed and how the necessary computations done by the controller are carried out. In this relation, it is important for the column flotation process to measure the controlled variables accurately and to identify how the interactions among the controlled and manipulated variables influence the dynamic performance of the whole system [2], [18]. The interactions between the manipulated and the controlled variables in the existing flotation processes deteriorate the performance of the used PI or PID controllers as their parameters are determined without taking into account the existence of these interactions. At the same time, it will be very expensive to remove all existing controllers and substitute them with more complex ones. This problem can be solved if in some way the influence of the interactions is taken into account during the process of the design of the PI controllers' parameters.

Thus, the paper proposes an improved method for the design of decentralised PI controllers that can handle all the possible errors, set-point tracking, and disturbance rejection by the introduction of an additional step of decoupling the model of the process into independent sub-models before the step of the design of the controller parameters. The influence of the interconnections is incorporated into the sub-models. In this way, the design of the controller parameters is based also on the values of the interconnections. This paper starts with the process modeling (section 2.1) and the decoupling of the column flotation process (section 2.2). Section 2.3 presents the design of fully decentralised PI controllers for each apparent loop of the decoupled system using the Pole Placement technique. Simulation results and their analysis are shown in section 3. Section 4 presents the conclusion of the paper.

2. FLOTATION PROCESS MODELLING AND DECENTRALISED CONTROLLERS DESIGN

The standard flotation column design is made up of two principal zones: the collection zone and the cleaning zone as shown in Figure 1, [10], [12]. Figure 1 is an illustration of the flotation column process, with the focus on the two zones (collection and cleaning). The process variables are: U_w is a pneumatic valve used to control the amount of the wash water flowrate Q_w measured using an electromagnetic flow meter; U_g is a pneumatic valve used to control the amount of air flow rate Q_g measured by a mass flow meter; U_T is a variable speed peristaltic pump used to control the non-floated fraction Q_T.

For control design, a dynamic model that indicates the dominant features of the flotation process operation is presented by (1). This is a mathematical model of the column flotation process as derived by [10].

$$\begin{bmatrix} h \\ \varepsilon_{gcz} \end{bmatrix} = \begin{bmatrix} G_{11} & G_{12} \\ G_{21} & G_{22} \end{bmatrix} * \begin{bmatrix} Q_W \\ Q_g \end{bmatrix} \quad (1)$$

Where *h* represents the froth layer height, ε_{gcz} is the air hold up variable, and *Q's* represent the flowrates. The detailed expressions of the transfer functions of G_{11}, G_{12}, G_{21}, G_{22} were identified and validated by [10]. The two transfer functions G_{11}, and G_{12} are related to the froth layer height. The transfer functions related to the air holdup process in the recovery zone are G_{21}, and G_{22}.

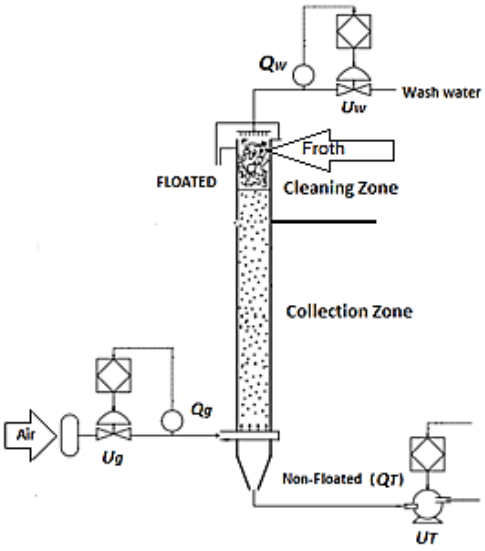

Figure 1. Schematic diagrams of the pilot flotation column and related instrumentation [10]

The froth layer height represented in Laplace domain is shown in (2):

$$h(s)=G_{11}(s)Q_w(s)+G_{12}(s)Q_g(s) \tag{2}$$

After substitution of the detailed expressions of the transfer functions from [10] into (2), the transfer function for the froth layer height is shown in (3)

$$\begin{aligned} h(s) &= \frac{-(1.029\times10^{-3}\,s+2.3\times10^{-5})}{(s+4.02\times10^{-4})(s+1.92\times10^{-2})}Q_w(s)+\left(\frac{-1.59\times10^{-4}\,s+4.33\times10^{-7}}{(s+4.02\times10^{-4})(s+7.98\times10^{-3}}\right)Q_g(s) \\ &= \frac{-1.029\times10^{-3}\,s-2.3\times10^{-5}}{s^2+19.602\times10^{-3}\,s+7.7184\times10^{-6}}Q_w(s)+\frac{-1.59\times10^{-4}\,s+4.33\times10^{-7})}{s^2+8.383\times10^{-3}\,s+3.208\times10^{-6}}Q_g(s) \end{aligned} \tag{3}$$

From (1) the Laplace representation of the air holdup model in the recovery zone is

$$\varepsilon_{gcz}(s)=G_{21}(s)Q_w(s)+G_{22}(s)Q_g(s) \tag{4}$$

After substitution of the detailed expressions of the transfer functions from [10] into (4), the transfer function for the air holdup is shown in (5)

$$\varepsilon_{gcz}(s)=\frac{7.6\times10^{-5}}{s+1.92\times10^{-2}}Q_w(s)+\frac{7.78\times10^{-5}}{s+1.92\times10^{-3}}Q_g(s) \tag{5}$$

The model of the column flotation process, presented by (3) and (5) is a built-in MATLAB/Simulink software environment as shown in Figure 2. The transition behaviour of the model is obtained. The characteristics of the model transition behaviour are given in Table 1. These characteristics are used later for the process closed-loop control design.

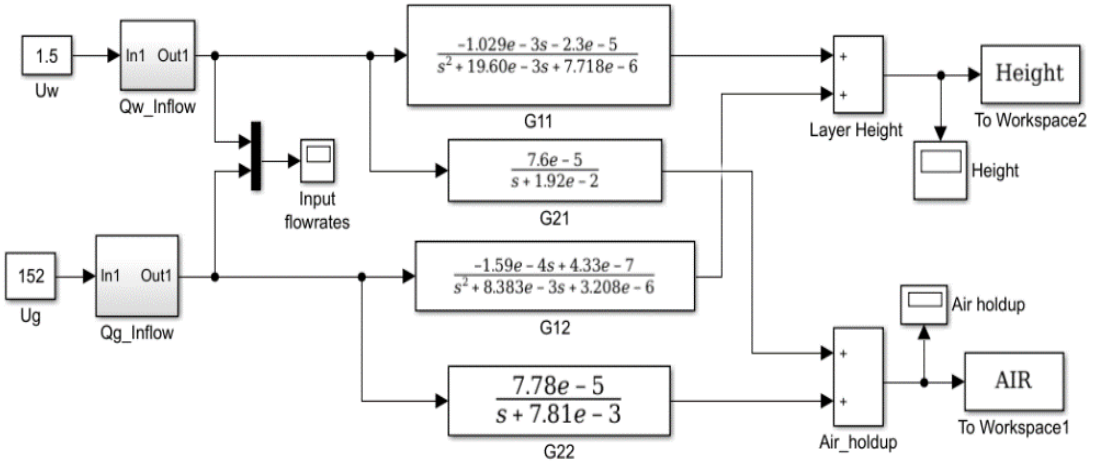

Figure 2. Simulink block diagram of the flotation process model

Table 1. Characteristics of the flotation process model response

Parameters	Height Value	Air holdup values
Rise Time	77 (min)	18 (min)
Settling time	116 (min)	22 (min)
Overshoot	0 (cm)	0.12 (%)
Peak	21.55 (cm)	0.44 (%)
peak time	133.33 (min)	128.67 (min)

The model given by (3) and (5) is interconnected and it is necessary to design decoupling controllers that will decouple the model into two independent sub-models allowing separate and simple industrial controllers to be designed and applied. The following section presents the process of decoupling the multivariable model presented in Figure 2 (given by (3) and (5)).

2.1. Decoupling of the multivariable column flotation model

Based on the advantages of minimisation of interactions between the input and output variables of the process, complete independence of the closed-loops can be achieved. This allows independent control of the individual loops by their respective designed controllers. The use of the dynamic decoupling method guarantees that under any operating conditions, the manipulated variables influence independently the particular controlled outputs [26]. This method is selected to be applied to design a decoupler of the column flotation model. Figure 3 represents a 2x2 column flotation closed-loop system model with a decoupling at the input of a plant model, and a controller's signals sent to the decoupled model.

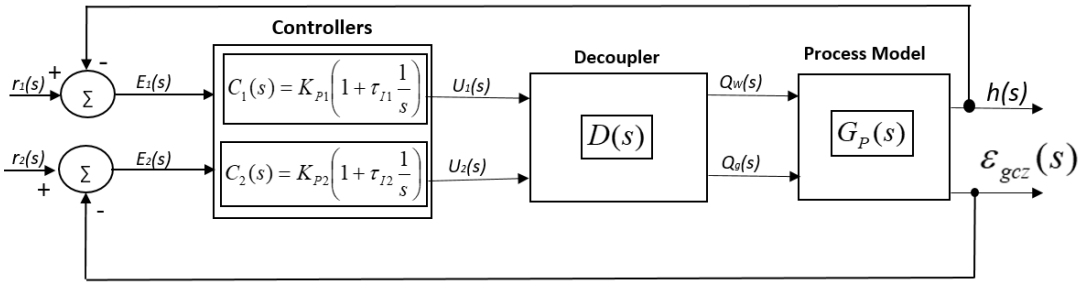

Figure 3. The decoupled controlled system

To achieve decoupling, the process model $G_p(s) \in R^{2x2}$ requires the design of a transfer function matrix $D(s) \in R^{2x2}$, such that $G_p(s) \bullet D(s)$ is a diagonal transfer function matrix $M(s) \in R^{2x2}$ [5], [25], [27] as shown in (6) and (7).

$$M(s)=G_P(s)\bullet D(s) \tag{6}$$

The decoupling strategy consists of setting a diagonal transfer function matrix for the representation of the decoupled process model making $M_{12}=M_{21}=0$, setting the diagonal elements of the decoupler to be 1, $D_{11}=D_{22}=1$, and then selecting the off-diagonal elements of $D(s)$ as presented in (7)-(10).

$$\begin{bmatrix} M_{11}(s) & 0 \\ 0 & M_{22}(s) \end{bmatrix}=\begin{bmatrix} G_{11}(s) & G_{12}(s) \\ G_{21}(s) & G_{22}(s) \end{bmatrix}.\begin{bmatrix} 1 & D_{12}(s) \\ D_{21}(s) & 1 \end{bmatrix} \tag{7}$$

Multiplication of the matrices in (7) produces (8):

$$\begin{bmatrix} M_{11}(s) & 0 \\ 0 & M_{22}(s) \end{bmatrix}=\begin{bmatrix} G_{11}(s)+G_{12}(s)*D_{21}(s) & G_{11}(s)*D_{12}(s)+G_{12}(s) \\ G_{21}(s)+G_{22}(s)*D_{21}(s) & G_{21}(s)*D_{12}(s)+G_{22}(s) \end{bmatrix} \tag{8}$$

The matrix at the right part of (8) has to be diagonal and to achieve this the $D_{12}(s)$ and $D_{21}(s)$ are selected to make the off-diagonal elements of the matrix on the right side of (8) to be zeros. From (8) for the matrix $M(s)$ to be diagonal, it can be written as (9):

$$\begin{aligned} &G_{11}(s)*D_{12}(s)+G_{12}(s)=0 \\ &G_{21}(s)+G_{22}(s)D_{21}(s)=0 \end{aligned} \tag{9}$$

Using (9), the mathematical expressions for $D_{12}(s)$ and $D_{21}(s)$ can be derived (10):

$$D_{12}(s)=-\frac{G_{12}(s)}{G_{11}(s)};\quad D_{21}(s)=-\frac{G_{21}(s)}{G_{22}(s)} \tag{10}$$

The decoupled model of the process is obtained by substituting the dynamic decouplers given by $D_{21}(s)$ and $D_{12}(s)$ from (10) into (8) and the following equation is obtained (11):

$$\begin{bmatrix} M_{11}(s) & 0 \\ 0 & M_{22}(s) \end{bmatrix}=\begin{bmatrix} G_{11}(s)-\frac{G_{21}(s)}{G_{22}(s)}G_{12}(s) & 0 \\ 0 & G_{22}(s)-\frac{G_{21}(s)G_{12}(s)}{G_{11}(s)} \end{bmatrix} \tag{11}$$

The diagonal elements in (11) represent the transfer functions of the decoupled model of the column flotation process. These transfer functions are used for the design of decentralized controllers for this process with highly minimized interactions. Based on (11) it can be seen that the decoupled model of the froth layer height is as shown in (12):

$$h(s)=M_{11}(s)=G_{11}(s)-\frac{G_{12}(s)G_{21}(s)}{G_{22}(s)} \tag{12}$$

and the decoupled model of the air holdup is shown in (13):

$$\varepsilon_{gcz}(s)=M_{22}(s)=G_{22}(s)-\frac{G_{21}(s)G_{12}(s)}{G_{11}(s)} \tag{13}$$

The detailed transfer functions of the model of the column flotation are substituted in (12) and (13) and their detailed transfer functions are obtained. The order of these transfer functions is high as they contain many zeros and poles and a reduction of them is necessary. The aim is to obtain simpler lower-order transfer functions to facilitate easier controller design as proposed in [5], [25], [27]. This is achieved through factorisation and simplification of the obtained decoupled detailed transfer functions. Transfer function substitution and simplification of the froth layer height decoupled model in (12), produces the following arrays of zero-pole-gains as (14):

$$M_{11}(s)=\frac{-0.00087368(s+0.02686)(s+0.0192)(s+0.007964)(s+0.000402)}{(s+0.0192)(s+0.0192)(s+0.007981)(s+0.000402)(s+0.000402)} \quad (14)$$

From the derived transfer function $M_{11}(s)$, it is noticed that the zeros in the numerator polynomial represented by (s+0.02582)(s+0.0192)(s+0.007991)(s+0.000402) can be cancelled with the poles of the denominator polynomial represented by (s+0.0192)(s+0.0192)(s+0.007981)(s+0.000402), resulting in a simplified transfer function as shown in (15).

$$M_{11}(s)=\frac{-873.68\times10^{-6}}{s+0.000402} \quad (15)$$

The same technique is followed to simplify the decoupled model of the air holdup. The following transfer function is obtained.

$$\varepsilon_{gcz}(s)=\frac{6.6057\times10^{-5}(s+0.02686)(s+0.0192)(s+0.007964)(s+0.000402)}{(s+0.02235)(s+0.0192)(s+0.007981)(s+0.00781)(s+0.000402)} \quad (16)$$

Cancelation of the numerator and denominator polynomials of similar terms in the above equation results in (17):

$$\varepsilon_{gcz}(s)=M_{22}(s)=\frac{6.6057\times10^{-5}}{s+0.00781} \quad (17)$$

Combining (15) and (17) into a matrix results to $M(s)$ as:

$$M(s)=\begin{bmatrix} M_{11}(s) & 0 \\ 0 & M_{22}(s) \end{bmatrix}=\begin{bmatrix} \frac{-873.68\times10^{-6}}{s+0.000402} & 0 \\ 0 & \frac{6.6057\times10^{-5}}{s+0.00781} \end{bmatrix} \quad (18)$$

The matrix $M(s)$ represents the decoupled model of the column flotation process and it is used for the design of the decentralized PI controllers for the individual decoupled loops of the flotation process.

2.2. Flotation process decentralised controllers design using the pole placement technique

Pole Placement is a technique that is applied in the feedback control system theory to place the closed-loop poles of a plant in pre-determined positions in the s-plane [28]. Once the closed-loop system transfer function is defined mathematically, the desired transfer function can also be defined, then for each coefficient of the same order in the closed-loop polynomials of these functions can be compared and the values of the controller parameters can be determined [28]. This arrangement control strategy comes about within the desired system response and is easy to mathematically find the controller gains [25], [28], [29]. The correctness or precision of the closed-loop system transfer function is essentially vital and it is costly to implement this method for high order systems, hence reduction of the system order is necessary [23].

2.2.1. PI controller design for the decoupled model of the froth layer height process

This subsection describes the PI controller design for the froth layer height $h(s)$. The following second-order transfer function (19) represents the closed-loop model of the froth layer process.

$$h(s)=\frac{C_1(s)M_{11}(s)}{1+C_1(s)M_{11}(s)}*r_1(s)$$
$$h(s)=\frac{-873.68e^{-6}(K_{P1}s+K_{P1}K_{I1})}{s^2+(0.000402-873.68e^{-6}K_{P1})s-873.68e^{-6}K_{P1}K_{I1}}*r_1(s) \quad (19)$$

The characteristic polynomial equation of the closed-loop transfer function contains the unknown parameters of the PI controller as shown in (20).

$$s^2 + (0.0004002 - 873.68e^{-6}K_{P1})s - 873.68e^{-6}K_{P1}K_{I1} = 0 \quad (20)$$

The values of the closed-loop system poles can be determined by a selection of appropriate values of the PI controller parameters K_{P1} and K_{I1}. Based on this requirement the proper values of the controller parameters can be selected if the desired values of the poles of the closed-loop system are selected [30]. A second-order standard desired dimensionless polynomial form determining the desired position of the closed-loop poles is compared with the characteristic polynomial of the closed-loop transfer function [25] as given in (21).

$$s^2 + (0.0004002 - 873.68e^{-6}K_{P1})s - 873.68e^{6-}K_{P1}K_{I1} = s^2 + 2\xi\omega_n s + \omega_n^2 \quad (21)$$

Where ξ and ω_n are the damping factor and the undamped natural frequency. Determination of the PI controller parameters is done through comparison of the coefficients in front of the equal powers of the Laplace variable. Therefore, the controller parameters are found as:

$$K_{P1} = \frac{2\xi\omega_n - 0.0004002}{-873.68e^{-6}} \quad (22)$$

$$K_{P1}K_{I1} = \frac{\omega_n^2}{-873.68e^{-6}} \quad (23)$$

To determine the required damping factor and un-damped natural frequency, the required settling time and the overshoot percentage of the closed-loop system have to be defined [31]. These are taken from the literature and are selected to be as follows: the peak value of the height is 21.55 cm and the settling time is 116 minutes [11]. The required desired values of the damping factor and the un-damped natural frequency are calculated below and in this way, the designed closed-loop system will have the required behaviour in terms of set-point tracking and disturbance rejection. The allowed maximum overshoot is selected to be M_{pmax}=15% of the peak value which is equivalent to 3.2 cm and the minimum overshoot value is selected to be M_{pmin}=5%, which is equivalent to 1.08 cm. The damping factor (ξ) can be calculated using (24) and (25). The maximum value of the damping factor is:

$$\zeta_{p\max} = \sqrt{\frac{\left(\ln\frac{M_{p\max}}{100\%}\right)^2}{\pi^2 + \left(\ln\frac{M_{p\max}}{100\%}\right)^2}} = \sqrt{\frac{\left(\ln\frac{3.2}{100\%}\right)^2}{\pi^2 + \left(\ln\frac{3.2}{100\%}\right)^2}} = 0.739 \quad (24)$$

And the minimum value of the damping factor is:

$$\zeta_{pmim} = \sqrt{\frac{\left(\ln\frac{M_{p\min}}{100\%}\right)^2}{\pi^2 + \left(\ln\frac{M_{p\min}}{100\%}\right)^2}} = \sqrt{\frac{\left(\ln\frac{1.08}{100\%}\right)^2}{\pi^2 + \left(\ln\frac{1.08}{100\%}\right)^2}} = 0.82 \quad (25)$$

Therefore, for each value of the allowed overshoot, the constraints of the damping factor are specified as shown in (26).

$$\begin{aligned} M_{p\max} &= 15\% \rightarrow \xi_{p\max} = 0.74 \\ M_{p\min} &= 5\% \rightarrow \xi_{p\min} = 0.82 \end{aligned} \quad (26)$$

The value of the damping factor is chosen to be ξ=0.8. The determination of the undamped natural frequency (ω_n) is done based on (27) [30].

$$T_s = \frac{4}{\xi \omega_n}; \tag{27}$$

This indicates that:

$$\omega_n = \frac{4}{T_s \xi} = \frac{4}{116 \times 0.8} = 0.043 rad/s \tag{28}$$

Therefore, the values of the unknown controller parameters are calculated as (29):

$$K_{P1} = \frac{2\xi\omega_n - 0.0004002}{-0.00087368} = \frac{(2 \times 0.8 \times 0.043) - 0.000402}{-0.00087368} = -78.3$$
$$K_{I1} = \frac{\omega_n{}^2}{-0.00087368\ K_{P1}} = \frac{(0.05)^2}{(-0.00087368) \times (-102.55)} = 0.027 \tag{29}$$

2.2.2. PI controller design for the decoupled model of the air holdup process

This subsection describes the PI controller design for the air holdup process. To form a closed-loop, the general decoupled (18) is used. The transfer function of the closed-loop Air hold up is (30):

$$\varepsilon_{gcz}(s) = \frac{6.6057e^{-5}(K_{P2}s + K_{P2}K_{I2})}{s^2 + (0.00781 + 6.6057e^{-5}K_{P2})s + 6.6057e^{-5}K_{P2}K_{I2}} * r_2(s) \tag{30}$$

The characteristic polynomial equation of the closed-loop transfer function contains the unknown parameters of the PI controller as (31).

$$s^2 + (0.00781 + 6.6057e^{-5}K_{P2})s + 6.6057e^{-5}K_{P2}K_{I2} \tag{31}$$

Where the controller parameters are K_{P2} and K_{I2}. In the same way, as for the first controller, a second-order standard desired dimensionless polynomial form determining the desired position of the closed-loop poles is compared with the characteristic polynomial of the closed-loop transfer function is given in (32).

$$s^2 + (0.00781 + 6.6057e^{-5}K_{P2})s + 6.6057e^{-5}K_{P2}K_{I2} = s^2 + 2\xi\omega_n s + \omega_n{}^2 \tag{32}$$

The procedure used to design the controller parameters in point 2.4.1 is applied again for the PI controller for the air holdup process. The peak value of the air holdup is 0.44% and the settling time is 22 minutes. The allowed maximum overshoot is selected to be M_{pmax} = 15% of the peak value which is equivalent to 0.065% and the minimum overshoot value is selected to be M_{pmin} = 5 %, which is equivalent to 0.022%. The damping factor (ξ) can be calculated using (24) and (25). The calculated maximum and minimum values of the damping factor are 0.92 and 0.937 respectively. The value of the damping factor is selected to be ξ= 0.92. The determination of the undamped natural frequency (ω_n) is done based on (27) and is found to be (33):

$$\omega_n = \frac{4}{T_s \zeta} = \frac{4}{22 \times 0.92} = 0.2\, rad/s \tag{33}$$

The values of the unknown parameters of the PI controller are calculated as given in (34):

$$K_{P2} = \frac{2\xi\omega_n - 0.00781}{6.60557e^{-5}} = \frac{(2\times 0.9\times 0.2) - 0.00781}{6.60557e^{-5}} = 5332$$
$$K_{I2} = \frac{\omega_n{}^2}{6.6057e^{-5}K_{P2}} = \frac{(0.2)^2}{6.6057e^{-5}\times 5332} = 0.11 \quad (34)$$

The procedure necessary to be followed for the design of the parameters of the controllers for the decoupled model of the process is illustrated in Figure 4. The simulation of the closed-loop column flotation system is given in the following section to investigate the importance of the application of the decouplers in a system with interactions.

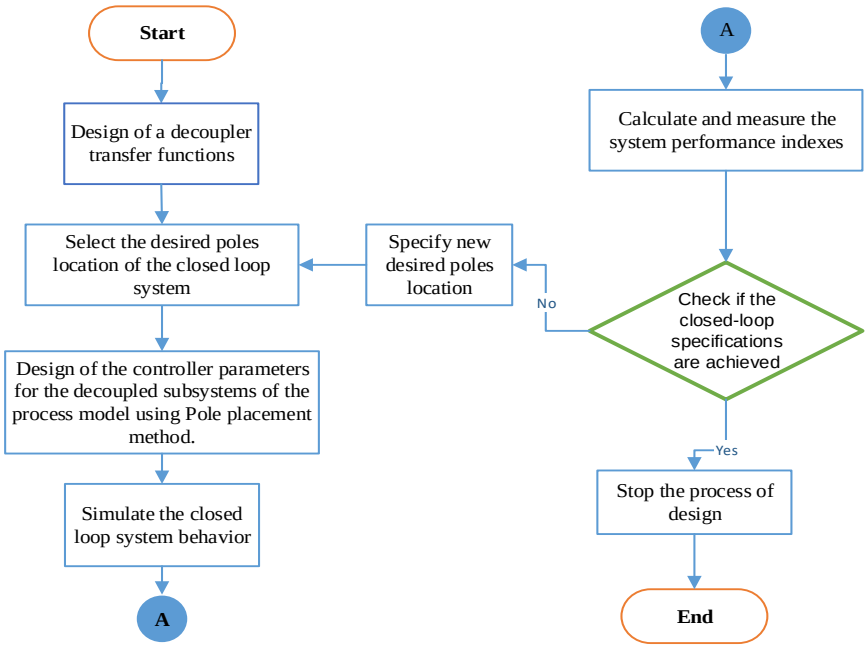

Figure 4. Flow-chart of the process of the decoupler and the controller designs

3. RESULTS AND ANALYSIS

3.1. Simulation and transition behaviour evaluation of the coupled and decoupled closed-loop systems

To investigate the effect and importance of decoupling in the multivariable systems, two closed-loop systems under the designed PI controllers are built and modeled in MATLAB/Simulink. The scheme in Figure 5 shows the closed-loop PI controlled system without a decoupler and Figure 6 shows the closed-loop decoupled system under the same PI controllers. Investigations on the behaviour of the two closed-loop systems are performed in MATLAB/Simulink to check the capabilities of the system for set-point tracking. Table 2 introduces the study cases for various set-points values which are the same for both systems. The setpoints of $h=60\ cm$ and $\varepsilon_{gcz}=18\%$ as tabled below are used as the first case study of the investigations.

3.2. Transition behaviour of the coupled closed-loop system under the decentralized PI controllers

An investigation conducted in this section for the set-point tracking by the coupled closed-loop system produced curves for its transition behaviours. MATLAB/Simulink simulations are performed for the coupled system given in Figure 5. The transition behaviour of the coupled closed-loop system under the designed decentralised PI controllers are presented from Figures 7 to 9, for the considered cases in Table 2 case studies.

Case study 1 corresponds to the data from the first row of Table 2. It can be seen from Figure 7 that the froth layer height process becomes unstable and the air holdup process follows the behaviour of the setpoint but cannot reach it in a steady-state. The steady-state error is 0.28%. Case study 2 corresponds to the data from the second row of Table 2. It can be seen from Figure 8 that the froth layer process behavior is worse than in the first Case study as the process behaviour is characterised by overshoot and instability. It can be noted that the peak overshoot of the froth layer height in the coupled system is not successfully or

smoothly controlled under the designed PI control parameters. The air holdup process follows the setpoint changes but again with a steady-state error of 0.33%. It can be observed that the frequent change of the setpoints destabilizes the flotation process behaviour. Case study 3 corresponds to the data from the third row of Table 2. The transition behavior of both processes is very similar to the second Case study–unstable and with steady-state errors.

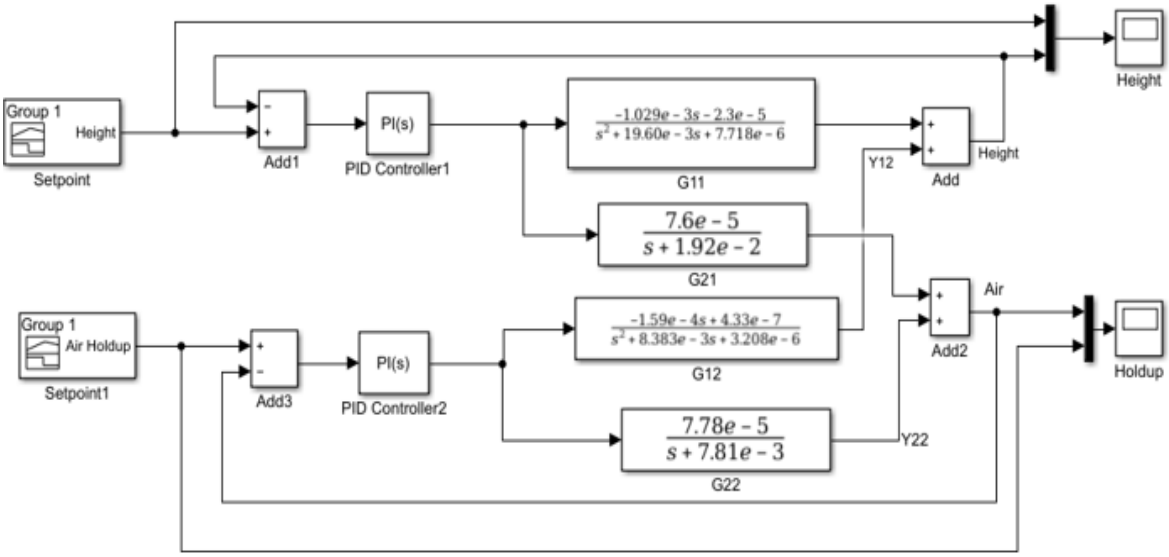

Figure 5. Block diagram of the closed-loop coupled system without a decoupler

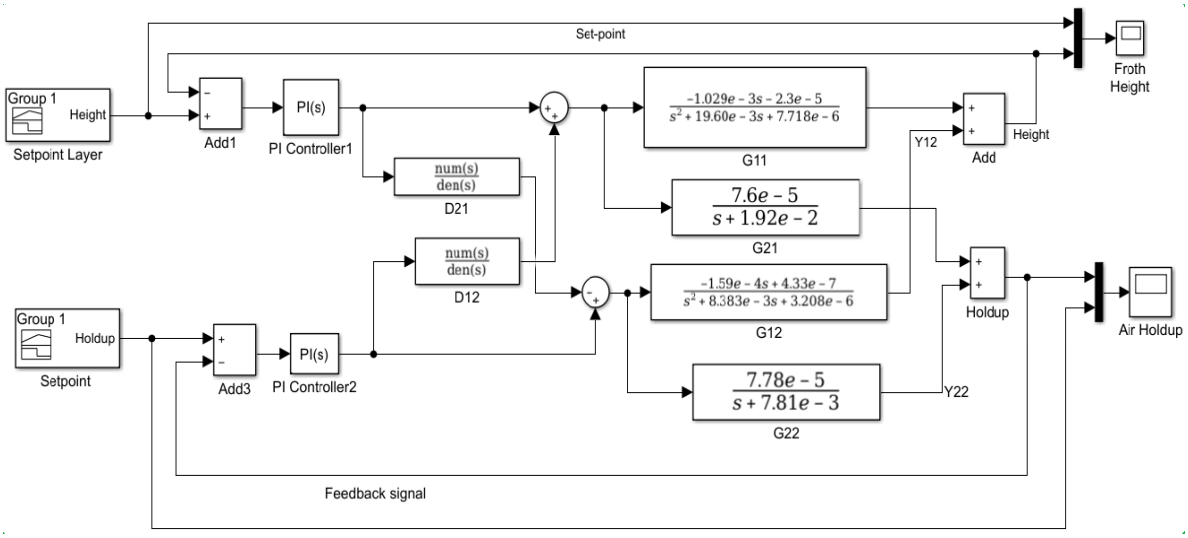

Figure 6. Block diagram of the closed-loop decoupled system

Table 2. Set-points following studies for the coupled and decoupled closed-loop systems

Study Case	Set-point		Coupled and Decoupled processes with PI controllers	
	h	ε_{gcz}	Froth Layer Height (cm)	Air holdup (%)
1	40-60 (cm)	10-18 (%)	Step change of the setpoint from 40 to 60 (cm)	Step change of the set point from 10 to 18(%)
2	50-70-60 (cm)	15-20-12 (%)	Step changes of the setpoint from 50 to 70 to 60 (cm)	Step changes of the setpoint from 15 to 20 to 12(%)
3	80-70-80 (cm)	20-15-20 (%)	Rectangular pulse change of the setpoint	Rectangular pulse change of the setpoint

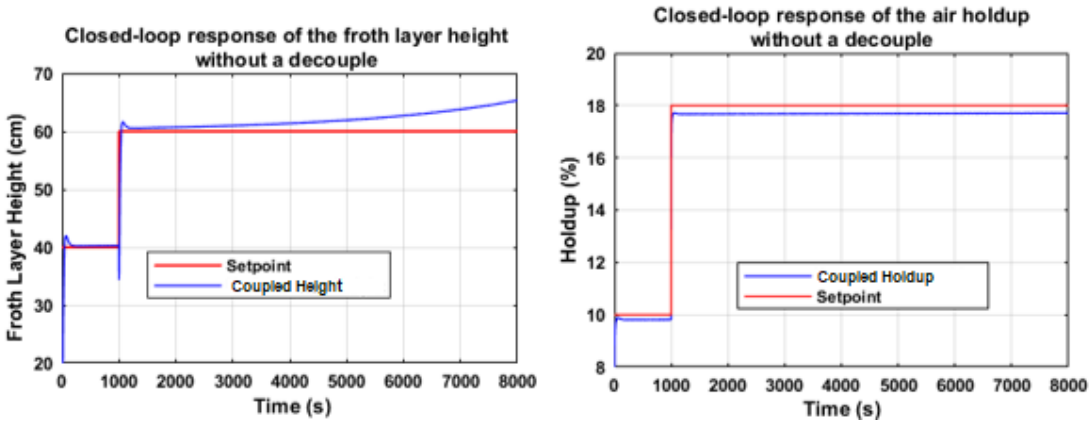

Figure 7. Case 1: Closed-loop response of the coupled froth layer height and air holdup processes

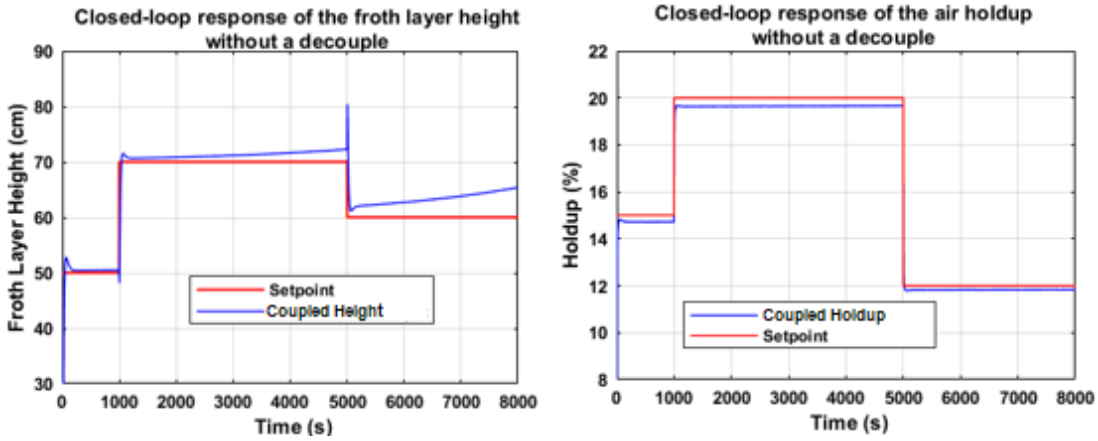

Figure 8. Case 2: Closed-loop response of the coupled froth layer height and air holdup processes

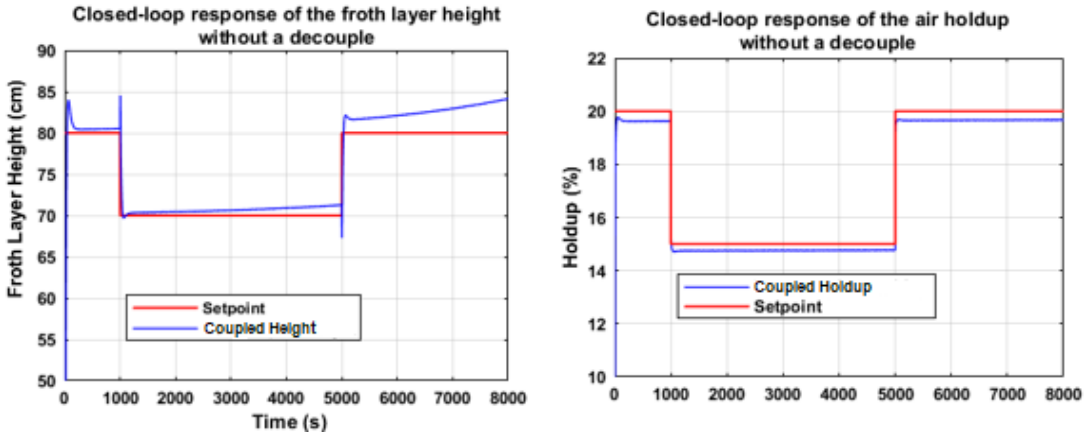

Figure 9. Case 3: Closed-loop response of the coupled froth layer height and air holdup processes

The characteristics of the transition behaviour of the coupled closed-loop system for the considered case studies are shown in Table 3. The investigation results show that the trajectories of the froth layer height and air holdup behaviour follow the set-point variations. It can be seen that the rise time has small values, but the settling time is high as the closed-loop system becomes unstable and the steady-state errors for the froth layer height are growing. The conclusion is that the designed decentralized PI controllers cannot successfully control the flotation process if it has interconnections between the manipulated and controlled variables

which are not decoupled. The next subsection of the paper presents the transition behaviour of the decoupled closed-loop system for the same case studies as above. Analysis and comparison of the results of the coupled and decoupled closed-loop responses are also presented.

3.3. Transition behaviour of the decoupled closed-loop system under the decentralized PI controllers

The simulation results are obtained for the decoupled closed-loop system shown on Figure 6. The same case studies from Table 2 are considered and the transition behaviours of the decoupled closed-loop system under the decentralized PI controllers are presented by Figures 10 to 12. For case study 1 the transition behavior of the decoupled system given by Figure 10 is different from this given by Figure 7 for the coupled system. Both processes-the froth layer height and the air holdup are stable and strictly follow the setpoint changes. The rising time is approximately the same as for the coupled system but the settling time is smaller than this of the coupled system. The steady-state error is smaller a couple of times.

For case study 2 the transition behavior of the decoupled system given by Figure 11 is also different from this given by Figure 8 for the coupled system Looking at the signal changes as presented in Figure 11, the performance indices such as settling time, overshoot and steady-state error are minimised or much better for the decoupled system in comparison with the coupled ones presented in Figure 8. This further proves that the dynamic decoupling control design works well irrespective of the set-point value changes, especially in cases where minimisation of a steady-state error is very important.

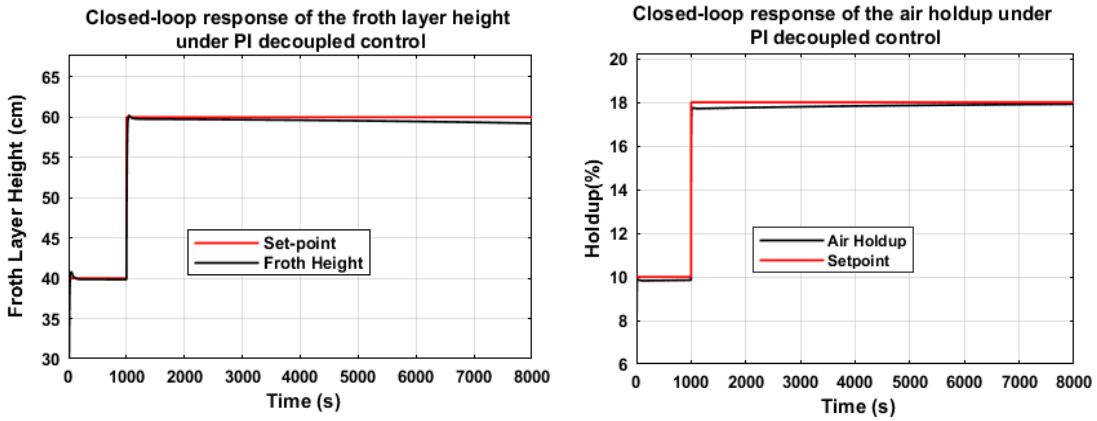

Figure 10. Case 1: Closed-loop response of the decoupled froth layer height and air holdup processes

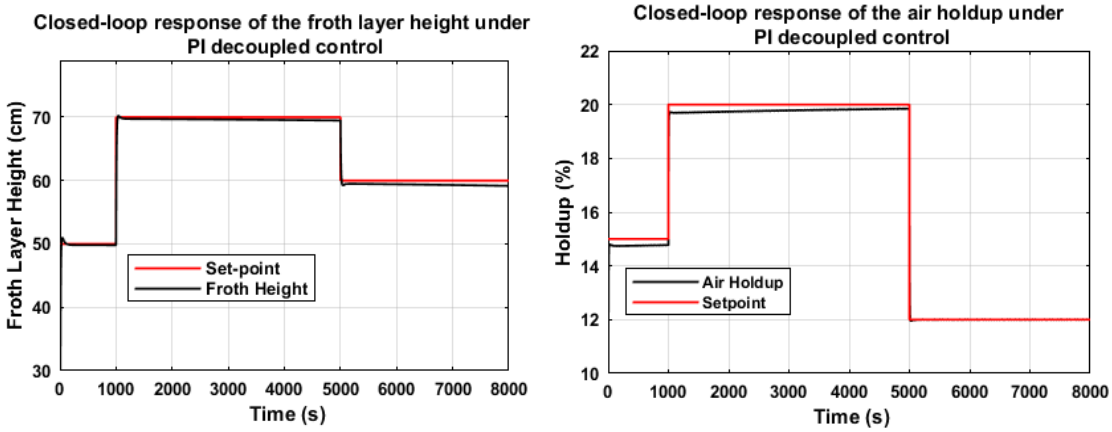

Figure 11. Case 2: Closed-loop response of the decoupled froth layer height and air holdup processes

For case study 3 the transition behavior of the decoupled system is given by Figure 12. Comparing the results in Figures 9 and 12, it can be noted that for the froth layer height and air holdup of the decoupled system the settling-time and steady-state error are again better than these for the coupled system. The

characteristics of the transition behaviour of the decoupled closed-loop system for the considered case studies are presented in Table 3. For all 3 cases, it can be noted that the decentralized PI controllers for both froth layer height and air holdup processes of the decoupled system performed a couple of times better than the decentralized PI controllers of the froth layer height and air holdup of the coupled system due to the additional action of the decouplers helping to compensate for the influence of the interconnections. On this basis, the control action of every one of the controllers affects only its controlled variable.

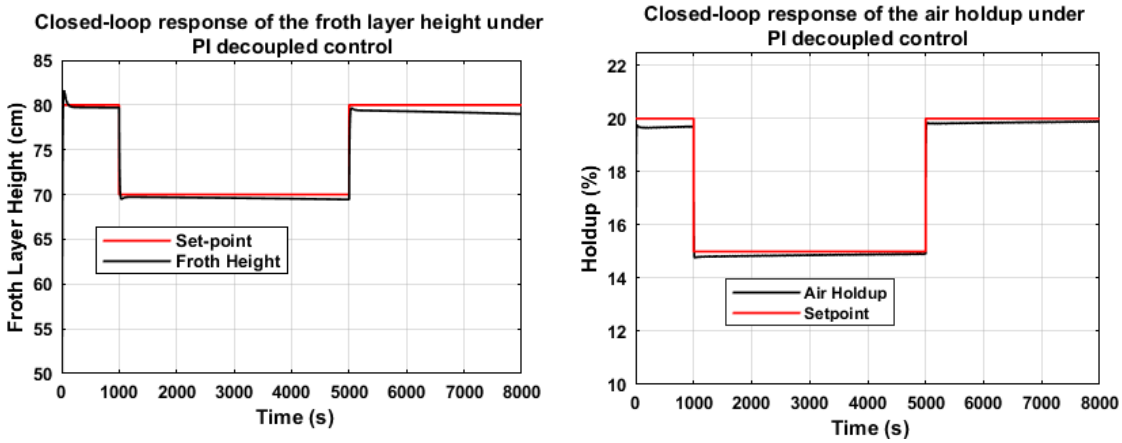

Figure 12. Case 3: Closed-loop response of the decoupled froth layer height and air holdup processes

Table 3. Transition processes performance indexes for the coupled and decoupled closed-loop systems

Case		Set-points	*Rise time [min]*	*Settling time [min]*	*Peak* M_P	*Steady-state error*
Characteristics of the Coupled Froth Layer Height and Air Holdup Processes						
1	h	40-60 (cm)	16.9	118	65.33 (cm)	5.3 (cm)
	ε_{gcz}	10-18 (%)	16.7	16.9	17.72 (%)	0.28 (%)
2	h	50-70-60 (cm)	16.7	118	80.4 (cm)	10.4 (cm)
	$\mathcal{E}_{gcz}$	15-20-12 (%)	0.36	83.6	19.67 (%)	0.33 (%)
3	h	80-70-80 (cm)	0.49	104	84.53 (cm)	4.53 (cm)
	$\mathcal{E}_{gcz}$	20-15-20 (%)	0.12	83.5	19.78 (%)	0.22 (%)
Characteristics of the Decoupled Froth Layer Height and Air Holdup Processes						
1	h	40-60 (cm)	16.8	17	60.25 (cm)	0.25 (cm)
	$\mathcal{E}_{gcz}$	10-18 (%)	16.7	16.9	17.92 (%)	0.08 (%)
2	h	50-70-60 (cm)	16.7	83.6	70.2 (cm)	0.2 (cm)
	$\mathcal{E}_{gcz}$	15-20-12 (%)	0.05	83.4	19.85 (%)	0.15 (%)
3	h	80-70-80 (cm)	0.24	83.5	81.20 (cm)	1.2 (cm)
	$\mathcal{E}_{gcz}$	20-15-20 (%)	0.1	83.45	19.89(%)	0.11 (%)

The next case study is performed to investigate the effects of the noise disturbance on the behavior of the froth layer height and air holdup respectively. The decoupled closed-loop system is disturbed at the output by injecting a noise disturbance in the Simulink diagram in Figure 6. Figure 13 presents the transition responses of these variables for setpoint tracking under disturbances with various magnitudes of 0.5 noise power for the froth layer height process and 0.1 noise power for the air holdup process. The results from the simulation show that the air holdup process is much more sensitive to the noise magnitude as bigger deviations of the transition behavior are obtained for smaller noise power in comparison with the froth layer height process. The simulations and the comparison of the obtained results show that the decentralized PI controller design based on dynamic decoupling is an effective strategy to be used irrespective of the set-point variations and disturbance influence. Decoupling of the model of the process has proven to be an effective strategy to reduce the influence of the interactions in the closed-loop control and consistently to keep the system stable.

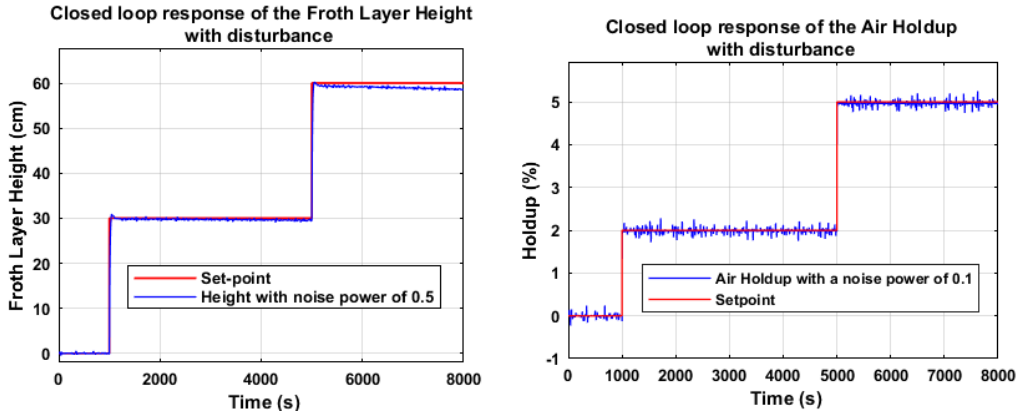

Figure 13. The closed-loop response of the froth layer height and air holdup processes in the case of disturbances at the process output

4. CONCLUSION

The performance of the flotation process is determined by the grade and recovery of the valuable mineral. This study focuses on the decentralized PI controller design for the column flotation processes. Based on the performed literature review, the fuzzy controllers still seem to be the best to control the column flotation process. However, the industry highly uses PI or PID controllers, because of their structural simplicity. They have been proven to be the most effective technology in engineering applications but for the case of the multivariable system, these controllers cannot overcome the influence of the interconnections between the manipulated and controlled variables. It is important to understand the relationship between the controlled and manipulated variables, to design proper controllers of this process. To overcome these difficulties this paper adopted the model decoupling based controller design strategy where the model of the process is decoupled in independent submodels through the introduction and design of decouplers and then decentralized PI controllers are designed for these submodels. The technique based on the pole-placement scheme is used for the decentralized PI controller design to achieve the desired set-point tracking performance and disturbance rejection. It has been made clear that pole placement designs do allow a decent closed-loop response, but require some experience to decide which pole locations are the best for any particular problem.

All results from the simulation of the closed-loop decoupled multivariable system have proven to be successful in set-point tracking and disturbance rejection. The comparison of the simulation results between the decoupled and non-decoupled (without decouplers) processes under the control of the same PI controllers' parameters shows that the performance of the decoupled system is better according to the obtained characteristics of the transition behaviour of these closed-loop systems. The obtained results will contribute to maintaining the existing PI controllers in the industry by enhancing their performance for multivariable systems using relevant design methods and simple decouplers which can be programmed in the existing PLCs. The future work will focus on the real-time implementation of this study using a PLC environment and real-time compact RIO simulation of the flotation process.

ACKNOWLEDGEMENTS

This work is supported by the THRIP/NRF project, "Centre for Substation Automation and Energy Management System (CSAEMS) development and growth", Reference No TP211061100004.

REFERENCES

[1] Y. Tian, M. Azhin, X. Luan, F. Liu, and S. Dubljevic, "Three-Phases Dynamic Modelling of Column Flotation Process," *IFAC PapersOnLine*, vol. 51, no. 21, pp. 99-104, 2018, doi: 10.1016/j.ifacol.2018.09.399.

[2] L. G. Bergh and J. B. Yianatos, "Flotation column automation: state of the art," *Control Engineering Practice*, vol. 11, no. 1, pp. 67-72, 2003, doi: 10.1016/S0967-0661(02)00093-X.

[3] B. J. Shean and J. J. Cilliers, "A review of froth flotation control," *International Journal of Mineral Processing*, vol. 100, no. 3-4, pp. 57-71, 2011, doi: 10.1016/j.minpro.2011.05.002.

[4] Z. Li, M. Huang, W. Gui, Y. Hua, and J. Zhu, "Optimal Reagents Control for Flotation Processes: An Adaptive Dynamic Programming Approach," *2019 Chinese Automation Congress (CAC)*, 2019, pp. 73-78, doi: 10.1109/CAC48633.2019.8997264.
[5] Y. Shen, W. J. Cai, and S. Li, "Multivariable Process Control: Decentralized, Decoupling, or Sparse?," *Industrial and Engineering Chemistry Research*, vol. 49, no. 2, pp. 761-771, 2010, doi: 10.1021/ie901453z.
[6] A. Antonyová and P. Antony, "Optimization the process of recycling the water contaminated with dispersion colorants," *2014 2nd International Conference on Technology, Informatics, Management, Engineering and Environment*, Indonesia, 2014, pp. 90-95, doi: 10.1109/TIME-E.2014.7011598.
[7] S. M. Vieira, J. M. C. Sousa, and P. O. Durao, "Combination of Fuzzy Identification Algorithms Applied to a Column Flotation Process," *2004 IEEE International Conference on Fuzzy Systems (IEEE Cat. No.04CH37542)*, Hungary, 2004, vol. 1, pp. 421-426, doi: 10.1109/FUZZY.2004.1375763.
[8] M. T. Carvalho and F. Durao, "Control of a flotation column using fuzzy logic inference," *Fuzzy Sets and Systems* vol. 125, no. 1, pp. 121-133, 2002, doi: 10.1016/S0165-0114(01)00048-3.
[9] A. Bahadori, G. Zahedi, S. Zendehnoudi, and M. Bahadori, "Estimation of air concentration in dissolved air flotation (DAF) systems using a simple predictive tool," *Chemical Engineering Research and Design*, vol. 91, no. 1, pp. 184-190, 2013, doi: 10.1016/j.cherd.2012.07.004.
[10] M. A. M. Persechini, F. G. Jota, and A. E. C. Peres, "Dynamic Model of a Flotation Column," *Minerals Engineering*, vol. 13, no. 14-15, pp. 1465-1481, 2000, doi: 10.1016/S0892-6875(00)00131-X.
[11] M. A. M. Persechini, A. E. C. Peres, and F. G. Jota, "Control strategy for a column flotation process," *Control Engineering Practice*, vol. 12, no. 8, pp. 963-976, 2004, doi: 10.1016/j.conengprac.2003.11.003.
[12] L. G. Bergh and A. R. Leon, "Simulation of Monitoring and Diagnosis of Flotation Columns Operation Using Projection Techniques," *Proceedings of the 44th IEEE Conference on Decision and Control*, Seville, Spain, 2005, pp. 7680-7685, 2005, doi: 10.1109/CDC.2005.1583402.
[13] D. Calisaya, E. Poulin, A. Desbiens, R. d. Villar, and A. Riquelme, "Multivariable Predictive Control of a Pilot Flotation Column," *2012 American Control Conference (ACC)*, Montréal, Canada, 2012, pp. 4022-4027, doi: 10.1109/ACC.2012.6315113.
[14] X. Xu, Y. Tian, Y. Yuan, X. Luan, F. Liu, and S. Dubljevic, "Output Regulation of Linearized Column Froth Flotation Process," *IEEE Transactions on Control Systems Technology*, vol. 29, no. 2, pp. 249-262, 2021, doi: 10.1109/TCST.2020.2974430.
[15] Y. Tang, C. Peng, S. Yin, J. Qiu, H. Gao, and O. Kaynak, "Robust Model Predictive Control Under Saturations and Packet Dropouts with Application to Networked Flotation Processes," *IEEE Transactions on Automation Science and Engineering*, vol. 11, no. 4, pp. 1056-1064, 2014, doi: 10.1109/TASE.2013.2283304.
[16] M. Maldonado, A. Desbiens, and R. del Villar, "Potential use of model predictive control for optimizing the column flotation process," *International Journal of Mineral Processing*, vol. 93, no. 1, pp. 26-33, 2009, doi: 10.1016/j.minpro.2009.05.004.
[17] A. Riquelme, A. Desbiens, R. del Villar, and M. Maldonado, "Predictive control of the bubble size distribution in a two-phase pilot flotation column," *Minerals Engineering*, vol. 89, pp. 71-76, 2016, doi: 10.1016/j.mineng.2016.01.014.
[18] V. Veselý and N. Q. Thuan, "Robust decentralized controller design for large scale systems," *12th International Carpathian Control Conference (ICCC)*, 2011, pp. 425-428, doi: 10.1109/CarpathianCC.2011.5945893.
[19] S. Mohanty, "Artificial neural network based system identification and model predictive control of a flotation column," *Journal of Process Control*, vol. 19, no. 6, pp. 991-999, 2009, doi: 10.1016/j.jprocont.2009.01.001.
[20] A. Faruq, M. F. N. Shah, and S. S. Abdullah, "Multi-objective Optimization of PID Controller using Pareto-based Surrogate Modeling Algorithm for MIMO Evaporator System," *International Journal of Electrical and Computer Engineering (IJECE)*, vol. 8, no. 1, pp. 556-565, 2018, doi: 10.11591/ijece.v8i1.pp556-565.
[21] M. Nafea, A. R. M. Ali, J. Baliah, and M. S. M. Ali, "Metamodel-based Optimization of a PID Controller Parameters for a Coupled-tank System," *TELKOMNIKA Telecommunication Computer Electronics and Control*, vol. 16, no. 4, pp. 1590-1596, 2018, doi: 10.12928/TELKOMNIKA.v16i4.9069.
[22] M. Tajjudin, M. A. A. Pani, S. A. Aziz, N. Ishak, and R. Adnan, "A Study on IMC-based PID for Steam Distillation Process," *2018 IEEE International Conference on Automatic Control and Intelligent Systems (I2CACIS)*, 2018, pp. 133-136, doi: 10.1109/I2CACIS.2018.8603701.
[23] B. A. Ogunnaike and W. H. Ray, "Process Modeling and Control," *A Series of Textbooks and Monographs*, 1994.
[24] G. He, J. Li, and P. Cui, "Decoupling Control Design for the Module Suspension Control System in Maglev Train," *Mathematical Problems in Engineering*, vol. 2015, pp. 1-13, 2015, Art. no. 865650, doi: 10.1155/2015/865650.
[25] R. Mittal and M. Bhandari, "Design of Robust PI Controller for Active Suspension System with Uncertain Parameters," *IEEE International Conference on Signal Processing, Computing and Control*, 2015, pp. 333-337, doi: 10.1109/ISPCC.2015.7375051.
[26] V. Kucere, "Decoupling optimal controllers," *Proceedings of the 18th International Conference on Process Control*, 2011, pp. 400-407.
[27] H. Vhora and J. Patel, "Design of Static and Dynamic Decoupler for Coupled Quadruple Tank Level System," *Nirma Univeristy Journal of Engineering and Technology*, vol. 5, no. 2, pp. 8-12, 2016.
[28] G. Suh, D. S. Hyun, J. I. Park, K. D. Lee, and S. G. Lee, "Design of a Pole Placement Controller for Reducing Oscillation and Settling Time in a Two-Inertia Motor System," *The 27th Annual Conference of the IEEE Industrial Electronics Society, IECON'01*, 2001, pp. 615-620, doi: 10.1109/IECON.2001.976556.
[29] S. Nadda and A. Swarup, "Decoupled control design for robust performance of quadrotor," *International Journal of Dynamics and Control*, vol. 6, pp. 1367-1375, 2018, doi: 10.1007/s40435-017-0380-0.

[30] S. N. Ahmadabad and S. Ghaemi, "The Design of Pole Placement With Integral Controllers for Gryphon Robot Using Three Evolutionary Algorithms," *International Journal of Materials, Mechanics and Manufacturing*, vol. 5, no. 2, pp. 127-131, 2017, doi: 10.18178/ijmmm.2017.5.2.303.
[31] K. Ogata, "Modern Control Engineering," *Pearson Education International, Fourth Edition*, Chapter 9-12, 2002.

BIOGRAPHIES OF AUTHORS

Nomzamo Tshemese-Mvandaba is a doctoral student in the Department of Electrical, Electronics and Computer Engineering, Cape Peninsula University of Technology (CPUT), Cape Town. She holds a degree of Master of Technology in Electrical Engineering from CPUT. Her research interest is in linear and non-linear multivariable system modeling, controller design, Process Instrumentation, and PLC applications.

Raynitchka Tzoneva has MSc and PhD in Electrical Engineering (control specialization) from the Technical University of Sofia (TUS), Bulgaria. She has been a lecturer at the TUS and an Associated Professor at the Bulgarian Academy of Sciences, Institute of Information Technologies between 1982 and 1997. Since 1998 she has been working as a Professor at the Department of Electrical, Electronic and Computer Engineering. R. Tzoneva's research interest is in the fields of optimal and robust control design and optimization of linear and nonlinear systems, energy management systems, real-time digital simulations, and parallel computation.

Mkhululi Elvis Siyanda Mnguni received a B-tech degree in Electrical Engineering from the Cape Peninsula University of Technology in 2006 and his Master degree from the Cape Peninsula University of Technology in 2014. Currently, employed as a Research Scholar and Lecturer. He completed his D-Eng. degree at the Cape Peninsula University of Technology in 2018. His research interests are Power system stability, protection, substation automation, process instrumentation and PLC applications.